UV Spectrum of the High Energy Conformer of 1,3-Butadiene in the Gas Phase

Jack Saltiel,* Donald F. Sears Jr., and Andrzej M. Turek*,†

Contribution from the Department of Chemistry, The Florida State University, Tallahassee, Florida 32306-4390

Received: April 19, 2001; In Final Form: June 4, 2001

Principal component analysis and singular value decomposition (PCA and SVD) with self-modeling (SM) based on the van't Hoff equation constraint, were applied to 1,3-butadiene UV spectra measured in the 5.0−93.0 °C range. The shape of the resolved UV spectrum of the high-energy conformer of 1,3-butadiene is sensitive to broadening of the spectra of the individual conformers with increasing *T*. A simulated spectral set, in which temperature broadening was purposely included, was used to develop a procedure that allows precise recovery of the pure component spectra. A set of Gaussians is derived that, on convolution with the spectrum for each corresponding *T*, creates a uniformly broadened spectral set. Exact recovery of the "s-cis spectrum" from the simulated spectral set is accomplished. Treatments of the experimental spectra using this method yields a minor conformer 1,3-butadiene spectrum that is only slightly red-shifted relative to the *s-trans*-1,3-butadiene spectrum and is consistent with the s-gauche structure. Application of PCA-SM to the onsets of the simulated spectral set showed that temperature broadening does not significantly alter the conformer enthalpy difference derived from the best-fit van't Hoff plot (compare 3.00000 kcal/mol assumed with 2.99992 kcal/mol recovered). The experimental onset spectra give $\Delta H° = 2.926$ kcal/mol, in excellent agreement with previously reported values.

Introduction

1,3-Butadiene is the prototypical example of molecules with conjugated double bonds, which by virtue of facile rotation about essential single bonds exist at ambient temperatures as equilibrium mixtures of s-trans and higher energy s-cis/s-gauche conformations.[1] Freely equilibrating ground state conformers give noninterconverting excited molecules with different physical properties and different decay channels, because electronic

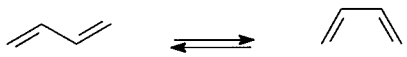

s-trans s-cis (1)

excitation in such systems, tends to reverse single/double bond order. Differences in conformer excitation energies and absorption spectra often lead to excitation wavelength, λ_{exc}, dependent populations of excited conformers and consequently to λ_{exc} controlled photochemical and photophysical responses. Control of photochemical response through selective excitation of ground state conformers was first postulated for 1,3,5-trienes related to vitamin D by Havinga, who generalized this concept in his principle of nonequilibrating excited rotamers (NEER).[2]

The adherence to the NEER principle in 1,3-dienes was first demonstrated by Hammond and co-workers in a study of the dependence of 1,3-diene dimer product ratios on the triplet donor excitation energy.[3] Conformer-specific 1,3-diene triplet reactivity was later demonstrated for triplet-sensitized cross-adduct formation[4] and for cis−trans photoisomerization.[5] Conformer specific singlet excited-state chemistry is also reflected in higher cyclobutene quantum yields from 1,3-dienes for which the s-cis conformer is more abundant.[6−8] Paradoxically, the photochemical interconversion of the conformers in eq 1 was observed in argon-matrix isolated 1,3-butadiene at 20 K.[9,10] Whether this reaction is an example of photoisomerization via the Hula-Twist process,[11] or occurs, at least in part, in the ground-state surface following internal conversion of the excited singlet state, remains to be established. In any case, 214 nm excitation of matrix isolated 1,3-butadiene shifts the conformer mixture toward the s-cis conformer allowing its characterization by IR and UV spectroscopy.[9,10] Other 1,3-dienes behave similarly.[12]

Determination of the absorption spectrum of each significant conformer, under the conditions of the experiment, is an essential first step in the quantitative elucidation of the photochemistry of 1,3-butadiene or other molecules exhibiting rotamerism. We have employed principal component analysis with self-modeling, PCA-SM, a method first described by Lawton and Sylvestre,[13] to decompose matrices of spectra reflecting different mixtures of a set of conformers. Because the method is based on the premise that the experimental spectra are linear combinations of a unique set of conformer spectra, it succeeds especially well with fluorescence spectra obtained for different λ_{exc} and quencher concentrations but in the same solvent and at constant *T*.[14] Use of PCA-SM to decompose spectra of mixtures of species whose composition is altered by changes in *T* (spectrothermal matrices) or medium must be conducted with great care in order to ensure that the results are not dominated by *T*-induced changes in the individual pure component spectra. PCA-SM can only hope to achieve accurate decomposition of the mixture spectra when nonlinear spectral changes in the spectra of the individual components are negligible relative to changes in the component composition. Applications of PCA-SM to spectrothermal matrices have led to resolutions of (a) the phosphorescence spectrum of platinum tetrabenzoporphyrin into two distinct spectra from different triplet sublevels[15] and (b) the luminescence of benzophenone in solution to phosphorescence and thermally populated delayed fluorescence spectra.[16]

PCA-SM attempts to resolve spectrothermal matrices of

†On leave from Jagiellonian University, Faculty of Chemistry, 30 060, Cracow, Poland.

10.1021/jp011493c CCC: $20.00
Published on Web 07/24/2001

mixtures of conformer absorption[17] and fluorescence[18] spectra measured in solution have failed.[19,20] Derived spectra, erroneously assigned as pure conformer spectra,[17,18] reflect primarily *T*-induced changes.[19,20] In solution, conformer spectra exhibit blue shifts and broadening as the temperature is increased, long recognized thermochromic phenomena.[21] Medium polarizability-dependent shifts in the spectra of conjugated hydrocarbons are especially troublesome because, since their magnitude depends on the oscillator strength of each electronic transition,[22] they do not affect the spectra of different conformers uniformly.[19,20] Recent attempts to develop methods that compensate for such effects,[23−25] have failed to yield a procedure that can be used to resolve spectrothermal matrices reflecting varying conformer composition.

In this work, thermally induced spectral shifts due to *T*-effects on medium properties (specifically, the index of refraction *n*) are eliminated by measuring the spectra in the gas phase, but variable thermal broadening is still a serious problem. Spectral broadening can be caused by properties inherent in the molecule, and/or by the spectrometer. Natural, collision and Doppler broadening are inherent in the gas-phase spectra of simple molecules.[26,27] However, contributions of collision and Doppler broadening to spectra of multiatomic molecules are usually of secondary importance, and consequently, other broadening mechanisms, such as internal conversion induced by nuclear motion,[28,29] photodecomposition,[30] isomerization,[31] and electronic-vibrational coupling with local and, for the liquid phase, long-range continuum modes,[32,33] have been considered.

Thermal broadening of vibronic bandwidths in the absorption spectra of simple polyenes was discussed in a comparison of the absorption spectra of jet-cooled *trans,trans*-octatetraene, *trans*-hexatriene and butadiene with corresponding room-temperature absorption spectra in the gas phase.[34] Thermal broadening contributes only about 15% to the overall broadening of the room temperature spectrum of 1,3-butadiene because the absorption spectrum of jet-cooled butadiene is inherently broad. The significantly narrower spectra of jet-cooled *trans*-hexatriene and *trans,trans*-octatetraene show well-resolved vibronic bands and much larger thermal broadening effects of 47% and 91%, respectively. The additional broadening in the room-temperature spectrum may be assigned to natural broadening, coupling of the 1^1B_u states with lower lying excited states (mostly with the closely lying 2^1A_g state), increased anharmonic coupling within the pure 1^1B_u manifold with excess vibrational energy or to increased involvement of very flat upper state potential surfaces in their internal conversion.[34] Among these possibilities, natural broadening is the one that best explains the dramatic increase in vibronic bandwidths with decreasing chain length. The rather short excited-state lifetime of hexatriene (~1.4 ns) together with a low fluorescence quantum yield ($<5 \times 10^{-5}$) can be associated with a natural line width of several hundred wavenumbers in the jet-cooled hexatriene absorption spectrum.[34] This effect should be more pronounced for the nonfluorescing butadiene system in view of its much shorter expected lifetime.

Because natural broadening is temperature independent, we are concerned here with the remaining sources of spectral broadening which depend on temperature. For instance, electronic-vibrational coupling in the strong coupling limit is known to give a square root *T* dependence of the bandwidth, becoming independent of *T* at very low temperatures.[35] Because the absorptivity at λ_{max} undergoes compensating variation, the oscillator strength remains constant. The derived functional dependence of the band envelope resembles in this case the Gaussian band shape, which is typical for the Doppler effect.[27] Similarly, in the weak coupling limit, a Lorentzian band shape at low *T* is postulated which may also become Gaussian at high *T*.[35]

A preliminary report of the PCA-SM based resolution of spectrothermal matrices of 1,3-butadiene UV spectra into s-trans and s-cis pure component spectra has been published.[36] In this paper, the effect of thermal broadening on the resolved spectra is evaluated by applying PCA-SM on a simulated spectral set. A procedure is developed that leads to excellent recovery of the assumed pure component spectra. The PCA-SM treatments of the 1,3-butadiene spectrothermal UV matrices are reported in detail and a new s-cis conformer spectrum is obtained using the procedure developed for the simulation.

Experimental Section

1,3-Butadiene (Aldrich, 99+%) was used as received. UV absorption spectra, measured using a Perkin-Elmer Lambda-5 spectrophotometer interfaced with a Dell Corp. 12-MHz 80286/87 microcomputer, were those reported earlier.[36] A jacketed 1 cm quartz cell was employed whose temperature was maintained to within ± 0.1 °C using a Haake FN constant temperature circulator. Temperatures were measured immediately above the light beam path with an Omega Engineering model 199*RT*D digital thermometer. The cell was flushed with Ar gas before introducing 1,3-butadiene vapor. Solid $CaCl_2$ was added to the bottom of the cell to avoid moisture condensation on the inner surfaces of the cell, and dry N_2 gas was used to flush the sample compartment and minimize condensation on the sample cell and instrument optics. Effects of photochemical reactions were avoided by frequent replacement of 1,3-butadiene vapor during the course of the measurements. Onset absorption spectra (matrix A) were recorded in 0.2 nm increments in the 220−265 nm range using a relatively high 1,3-butadiene partial pressure, ambient temperature absorbance = 1.79 at 225 nm. Measurements were performed at 18 temperatures between 5 and 92.9 °C. Spectra spanning the entire UV region (matrix B) were recorded in 0.4 nm increments in the 190−271 nm range employing a lower 1,3-butadiene partial pressure, ambient temperature absorbance = 1.90 at 215 nm. Measurements were performed at 18 temperatures between 8 and 93.0 °C. Both sets of spectra were recorded in quintuplicate for each *T*.

Results

The modified PCA-SM procedure was employed in this work.[14a] The effect of *T*-dependent spectral broadening on the resolution of conformer spectra was evaluated with the use of simulated spectral matrices, which were then used to develop a resolution method that takes broadening into account.

Simulated Ideal Spectra. A simulated spectrothermal data matrix that mimics the behavior of 1,3-butadiene was based on the two spectra in Figure 1. The Gaussian envelopes used to create the assumed *s-trans*-1,3-butadiene absorption spectrum were obtained by fitting to a low-temperature experimental spectrum. The spectrum for *s-cis*-1,3-butadiene (use of this name in this paper is not meant to distinguish between planar and gauche geometries) was arbitrarily chosen as an overlapping combination of one broad and two sharp bands, Table 1.

Mixture spectra, $\mathbf{y}_i$, were constructed as linear combinations of the $\mathbf{s}_{trans}$ (*s-trans*-1,3-butadiene spectrum) and the $\mathbf{s}_{cis}$ (*s-cis*-1,3-butadiene spectrum)

$$y_i = f_i s_{trans} + (1 - f_i) s_{cis} \qquad (2)$$

where f_i, the molar fractions of the s-trans conformer, obey the

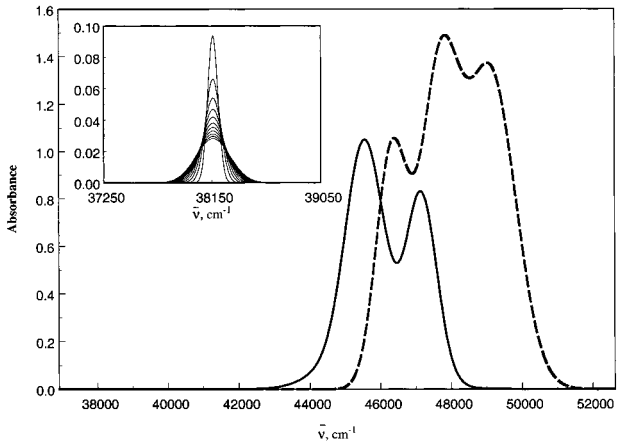

Figure 1. Simulated ideal spectra of *s-trans*- and *s-cis*-1,3-butadiene, dashed and solid lines, respectively; the inset shows temperature response functions used to model the broadened two-component 1,3-butadiene spectrothermal data matrix for $12.0 \leq T \leq 92.0$ °C.

TABLE 1: Band Parameters Used for the Ideal Spectrothermal Spectral Matrix

spectrum	band no.	height arbitrary units	width, nm	position, nm
s-trans	1	1.30	6.50	203.42
	2	1.35	5.75	209.55
	3	1.00	5.00	215.84
s-cis	1	0.75	4.50	212.00
	2	0.85	6.00	219.50
	3	0.20	12.00	222.00

van't Hoff equation

$$\ln\left(\frac{1-f_i}{f_i}\right) = -\frac{\Delta H^0}{RT_i} + \frac{\Delta S^0}{R} \tag{3}$$

The equilibrium in eq 1 was modeled by assuming $\Delta H° = 3.00$ kcal/mol and $\Delta S° = 3.1546$ eu, so that $f = 0.972$ at 20 °C. The spectrothermal data matrix consisted of 12 spectra at 8 °C intervals in the 4.0−92.0 °C range, covering the spectral range from 36 910 to 52 630 cm^{-1}.

Simulated Broadened Spectra. The mixture spectra for $T \geq 12.0$ °C were broadened by convolving each spectrum with a normalized Gaussian spread function of progressively increasing full width at half-maximum (fwhm). The convolution possesses the properties of commutativity and associativity, and is distributive with respect to addition.[27] The last property allows ideal spectra to be broadened separately and then added or, alternatively, added and then broadened as an ideal multicomponent spectral mixture. Thus, using the symbol ⊗ to denote convolution, we can write

$$b \otimes G = a \tag{4}$$

where b is the ideal spectrum, G represents the normalized Gaussian spread function, and a is the convolution product. The normalized Gaussian spread function has the form

$$G(\bar{\nu}) = \frac{1}{(2\pi)^{1/2}\sigma_G} \exp\left[-\frac{1}{2}\left(\frac{\bar{\nu}-m}{\sigma_G}\right)^2\right] \tag{5}$$

where m designates the mean wavenumber of the spread function and σ_G is the standard deviation, respectively. Convolutions were carried out using either the built-in MatLab 5.2 routine (conv.m) or the more sophisticated FFT-based convolution algorithms. The exact T dependence for band broadening in 1,3-butadiene is not known. The assumed dependence is similar to that characteristic for Doppler broadening and to strong electronic-vibrational coupling at high temperatures. Accordingly, the fwhm of a given Gaussian envelope varies with the square root of the temperature. Such dependence for absorption spectra measured under moderate gas pressure is rather typical and was employed by Mui and Grunwald to account for broadening in the Gaussian band assigned to the minor *s-cis*-1,3-butadiene component[37a] and in the analogous spectral component of isoprene.[37b]

When two Gaussian functions are convolved the variance (linearly related to the square of the fwhm) of the convolution product is the sum of the variances of the individual functions.[27] That is, when eq 4 holds true, we may write

$$\sigma_a^2 = \sigma_b^2 + \sigma_G^2 \tag{6}$$

It follows that for a given band the whole nonchemical temperature dependence (not connected with eq 3) is brought into the spectrum only by the spread function, meaning that a band reveals temperature dependent properties only upon convolution with the temperature variable response function. Thus, we have

$$\sigma_a^2 = \sigma_b^2 + \sigma_G^2(T) \tag{7}$$

In addition, because the area under the normalized spread function is unity, eq 4 represents a moving weighted average. This convenient constraint allows for visualization of the extent of the applied broadening with the temperature increase. For three temperatures such that $T_i < T_j < T_k$ we have

$$g_{ij} \otimes g_{jk} = g_{ik},\ G_i \otimes g_{ij} = G_j,\ G_j \otimes g_{jk} = G_k \text{ and } G_i \otimes g_{ik} = G_k \tag{8}$$

where g_{ij}, g_{jk}, and g_{ik} are the normalized relative-spread functions describing changes in broadening between corresponding pairs of temperatures T_i and T_j, T_j and T_k, and T_i and T_k, whereas G_i, G_j, and G_k are the effective spread functions actually applied to convolve with the spectra pertaining to temperatures T_i, T_j, and T_k. Thus, the standard deviation of all the relative spread functions depends on the difference of the related temperatures

$$\sigma_{ik} = k(T_k - T_i)^{1/2} \tag{9}$$

Once the single parameter k in eq 9 that relates the spectra in the set corresponding to the two lowest temperatures is determined, all other relative spread functions can be generated. The 11 effective spread functions, shown in the inset of Figure 1, were created using the property of associativity and each is a cumulative convolution product of the appropriate number of identical spread functions, because identical temperature intervals were employed in the simulation, eq 9. Because the lowest temperature spectrum was used as reference, it requires no broadening. The fwhm for the highest Gaussian response function depicted in Figure 1 was set at 100 cm^{-1}. The spacing between spectral points in cm^{-1} was the same as for the model ideal spectra (10 cm^{-1}), but the position of the Gaussian response profiles was arbitrarily set at 38150 cm^{-1} (abscissas do not enter directly into the convolution procedure).

Figure 2 shows the SVD derived eigenspectra (known also as eigenvectors) for the simulated spectrothermal matrices without (a) and with (b) broadening. Broadening causes significant changes in the shape of the second eigenspectrum, while leaving the shape of the first eigenspectrum almost unaltered. Furthermore, the broadened data matrix has additional significant eigenvalues and cannot be described as an exact two-

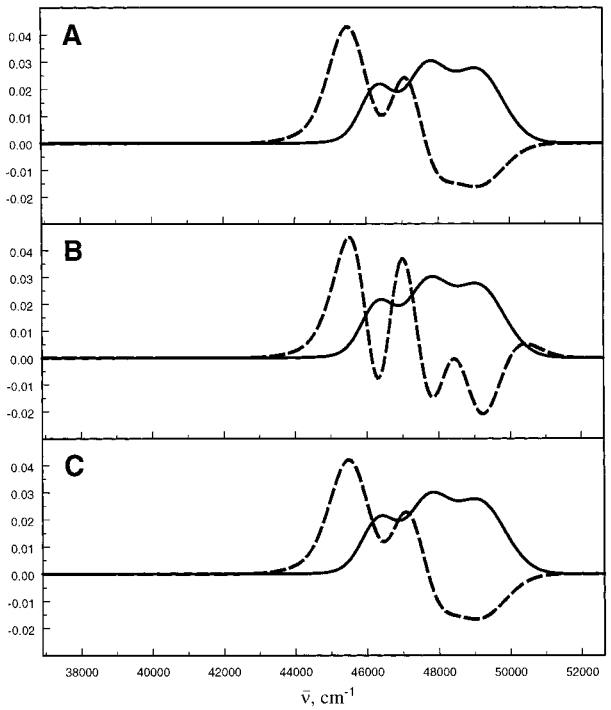

Figure 2. The first two significant eigenspectra for ideal (A), broadened (B), and compensated broadened (C) simulated data matrices.

component system. We describe below a procedure that allows recovery of pure component spectra from the thermally broadened simulated spectral matrix. It involves differentially broadening the spectra in order to create a uniformly broadened matrix corresponding to the broadening that applies to the spectrum for the highest T in the spectral set.

Uniform Broadening by Differential Compensation. Recovery of accurate pure component conformer spectra from a spectral matrix that includes thermal broadening could be achieved by SVD-SM or PCA-SM, if the lower temperature spectra were made to include the broadening applicable at the highest temperature of the data set. The aim is to construct a new spectrothermal matrix in which each spectrum is a convolution product of an ideal two-component spectrum and the same or nearly the same effective spread function. Treatment of such a matrix by SVD or PCA would then reveal only the variations due to differences in conformer composition.

Obviously, the differentially broadened simulated spectrothermal matrix can be converted to a matrix in which all spectra are uniformly broadened by convolution of the spectra with the same set of spread functions that was used in preparing the matrix, but in inverted order (resulting in maximum and minimum broadening of spectra for the lowest and penultimate temperatures, respectively). However, what is desired is a method that allows this process to be achieved without prior knowledge of the spread functions employed in the simulation. Assuming that the above scenario for thermal broadening is correct, i.e., that eq 9 describes the temperature dependence of effective spread functions, the task is reduced to deriving from the spectra the single parameter k in this equation.

Determination of the optimum value of k is based on SVD treatments of the set of spectral matrices generated from the initial matrix by successive trial compensations for broadening achieved by systematically stepping through a range of k values. Analysis of the evolution of the corresponding sets of eigenvalues reveals the value of k needed to generate the spread functions that exactly compensate for the differential broadening

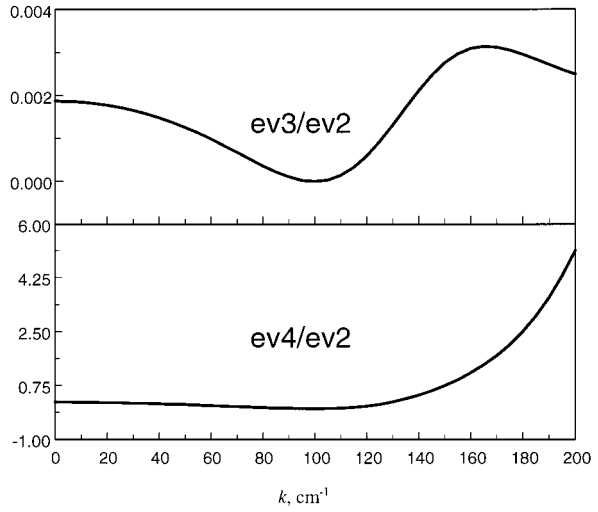

Figure 3. Ratios of eigenvalues as a function of compensating broadening (parameter k in eq 9) applied to the simulated broadened data matrix; ordinate values for ev4/ev2 are multiplied by 10^6.

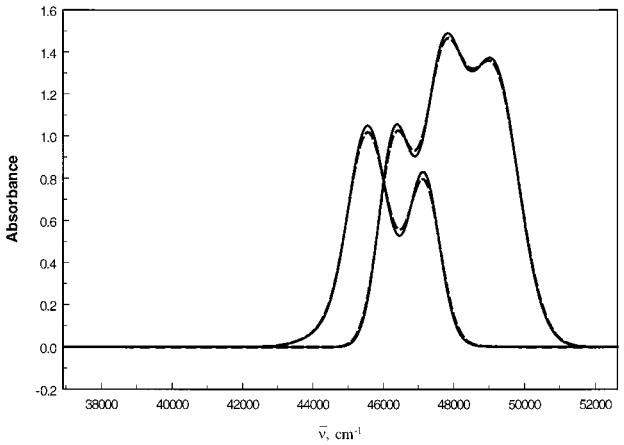

Figure 4. Recovered pure spectra for the ideal model data matrix (solid lines) and for the compensated broadened model data matrix (dashed lines).

in the simulated spectra. As can be seen in Figure 3, for the optimum value of k the third and fourth eigenvalues, plotted here as ratios to the second, become zero and the optimally broadened matrix becomes an exact two-component system. This is also evident, as expected, in Figure 2c where the shape of the second eigenvector of the compensated matrix is nearly identical to the second eigenvector of the ideal unbroadened matrix, Figure 2a. Because the spectra are uniformly broadened at the lowest and the highest temperature, for the initial and final matrix, respectively, the initial (Figure 2a) and final (Figure 2c) sets of eigenvectors correspond to exact two component systems that differ only in the extent of uniformly applied effective broadening. Identical pure component spectra are obtained based on Lawton and Sylvestre nonnegativity constraints or on optimization of the adherence of conformer contribution ratios to eq 3, the van't Hoff plot (see Appendix). These are shown in Figure 4 together with the input conformer spectra assumed in the simulation. The recovery is exact, as the derived spectra reflect only the difference in the assumed broadening for the highest and lowest temperature in the spectral set.

Inherent in this approach is the assumption that identical thermal spread functions apply to different vibronic/electronic bands within a conformer spectrum and to spectra of different conformers. This condition applies exactly to the differentially broadened spectra of our simulated matrix, but it is an assump-

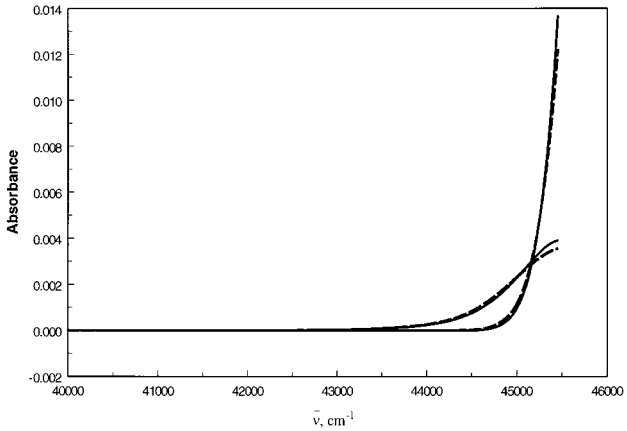

Figure 5. Normalized onset region spectra obtained for the uncompensated (solid lines) and compensated (dashed lines) broadened simulated spectrothermal matrices.

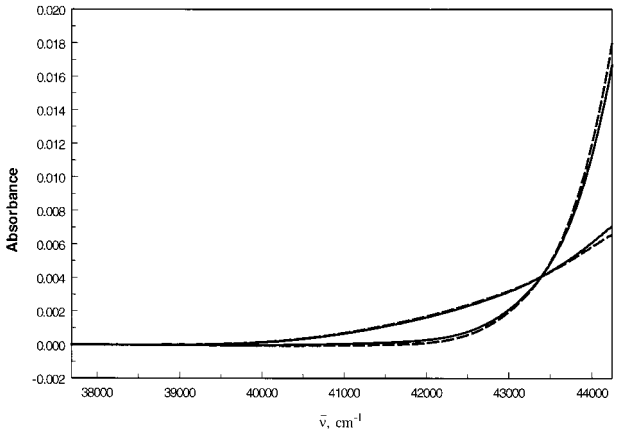

Figure 6. Pure component spectra obtained through PCA-SM with the van't Hoff constraint applied to the onset spectra of high-pressure samples of 1,3-butadiene: A_1 matrix (dashed lines) and A_2 matrix (solid lines).

tion when applied to experimental spectra. The effect of different sets of spread functions was evaluated by systematically varying k in eq 9 and applying the resulting sets of spread functions to the two ideal conformer spectra. Application of the above procedure to these spectral sets revealed that the broadening required to achieve optimally uniformly broadened spectral matrices is very close to that applied to the major component. Furthermore, the ratios of the first two eigenspectra obtained by SVD of spectral sets composed of differentially broadened conformer spectra reveals a minimum in the onset spectral region whose amplitude decreases as the difference between the assumed k is decreased, vanishing entirely when the conformer spectra are uniformly broadened. Thus, the behavior of the onset of the ratio of the two principal eigenvectors obtained by SVD treatment of broadening-compensated experimental matrices emerges as a test of the assumption that the same thermal broadening influences the spectra of the different conformers. When the difference in the k values for the two conformers is large, application of the above procedure to the simulated spectral matrix gives excellent recovery of the spectrum of the major component, and the recovered minor component spectrum retains its major spectral features, but is somewhat distorted.

Simulated Onset Spectra. In the preliminary report of this work, it was concluded that analysis of onset spectra recorded for the higher 1,3-butadiene vapor pressure (set A) provides a very satisfactory estimation of $\Delta H°$ for conformer equilibration.[36] This conclusion is confirmed in this section by applying the analysis on a simulated onset spectral matrix constructed from partial spectra in the 220−271 nm range taken from the complete broadened data matrix. The compensated broadened onset data matrix was created in the same way. The 220−250 nm range of the pure component spectra obtained by our PCA-SM treatment of the broadened and compensated broadened onset spectral matrices (Figure 5) reveals small differences. The increased broadening present in the compensated data matrix is clearly reflected in the derived pure component spectra. Those retrieved from the compensated broadened matrix possess slightly lower intensities than those obtained directly from the uncompensated broadened spectral set. The resolved spectrum for the s-trans conformer for the uncompensated onset possesses several very small negative intensities around 44 500 cm^{-1} illustrating in general the technical problems involved in the analysis of broadened data matrices. Compensation for broadening in the onset spectra leads to insignificant improvement in the value of $\Delta H°$, compare $\Delta H° = 2.99992(57)$ kcal/mol with $\Delta H° = 2.99997(3)$ kcal/mol (uncertainties in parentheses, both at the 95% confidence level) for the uncompensated and the compensated broadened onset, respectively. Both values are nearly identical to the value assumed in the simulation.

Experimental Onset Spectra. The high-pressure absorption spectra of 1,3-butadiene (set A) were recorded in the 220−265 nm range. Direct PCA-SM treatment of a spectral matrix limited to the 226−250 nm range with the van't Hoff constraint, had yielded $\Delta H^0 = 2.950 \pm 0.002$ kcal/mol,[36] a value which should be essentially exact based on the analysis of the simulated onset spectra. A small uncertainty in this value is expected because it is sensitive to the choice of pure component combination coefficients for the s-trans conformer.

The spectral matrix was confined, in this work, to the 226−265 nm range because of signal saturation at lower wavelengths.[36] Spectra, recorded in quintuplicate for each temperature, were averaged, baseline corrected, converted to wavenumbers and interpolated using FFT and spline routines to produce a 656 × 18 spectral matrix. SVD analysis of the spectral matrix revealed that three low temperature (278.13, 281.75, and 286.91 K) spectra deviate noticeably from the α,β stoichiometric line. Because these spectra adhere closely to the normalization line, it is likely that their absolute intensity was affected by water condensation on the cell. Accordingly, the PCA-SM treatment was applied to all the 1,3-butadiene onset spectra, as before (A_1), and to a truncated spectral set (A_2) that excludes the three anomalous spectra. The conformer spectra obtained for the A_2 matrix are very close to those obtained earlier for the A_1 matrix (Figure 6).[36] As expected, broadening is reflected in small negative intensities in a broad range of the initial part (39 500−41 500 cm^{-1}) of the s-trans spectrum. The van't Hoff constraint derived $\Delta H° = 2.926 \pm 0.010$ kcal/mol value for the A_2 matrix is in excellent agreement with the value obtained from the A_1 matrix,[36] and with the earlier value of 3.02 ± 0.09 kcal/mol from the analysis of onset absorption spectra over a much wider temperature range (298−621 K) that assigned all absorption in the 237−249 nm region to the s-cis conformer.[37a]

Full Range Experimental Spectra. Application of the above procedure to the low pressure 1,3-butadiene spectra (set B) yielded a 1573 × 18 matrix with spectra spanning the 36 910−52 630 cm^{-1} range. The first two eigenvalues obtained by SVD treatment of this matrix are much larger than the rest, but the third and fourth are larger than those typically assigned to noise. The two major eigenvectors reveal the major features found in the eigenvectors for the simulated broadened data matrix (compare Figures 2 and 7). Departure from a pure two-

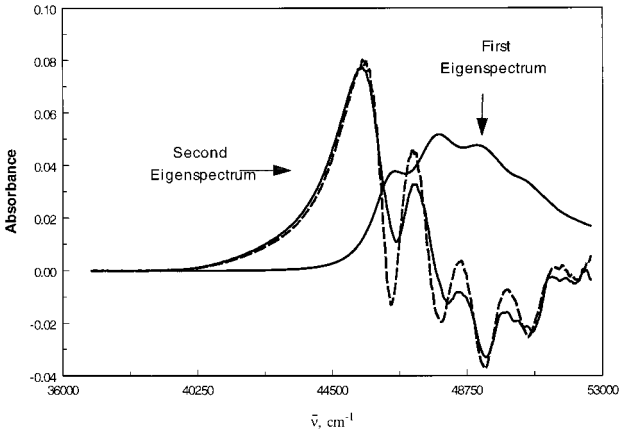

Figure 7. The first two SVD eigenvectors for the full-spectra matrix of 1,3-butadiene without (dashed lines) and with (solid lines) broadening compensation.

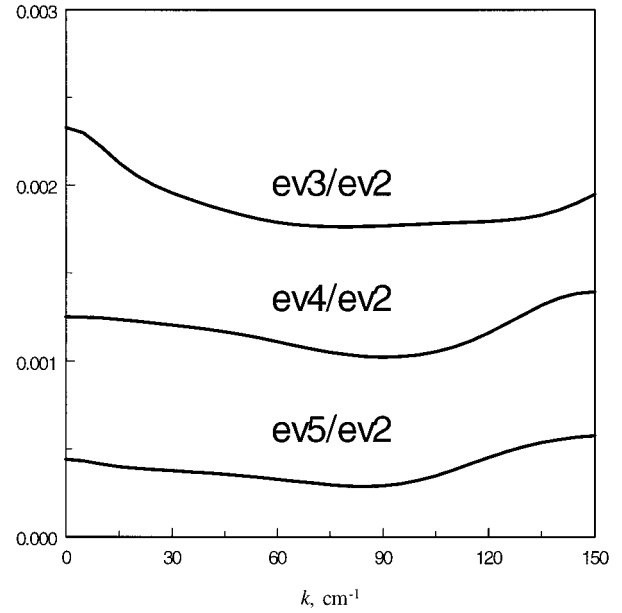

Figure 8. Evolution of eigenvalues as a function of fwhm (parameter *k* in eq 9) assigned to the first compensating spread function.

component system, evident in the third and fourth eigenvectors (not shown) and in the corresponding eigenvalues, is consistent with the influence of differential spectral broadening on the analysis.

The differential broadening compensation procedure was applied to the spectra as described for the simulated broadened spectral matrix. The eigenvalue evolution, as the value of *k* in eq 9 is varied (Figure 8), bears a strong qualitative resemblance to that observed for the simulated spectra (Figure 3). Relative changes in the third eigenvalue are most pronounced in both cases. All eigenvalue (ev) ratios in Figure 8 attain minimum values at nearly the same *k* (78, 90, and 85 cm^{-1}, for ev3/ev2, ev4/ev2, and ev5/ev2, respectively) but the wells are broader and shallower. That none of the minima is zero in Figure 8, reflects, at least in part, random noise in the experimental spectra, not modeled in the simulation. A more uniformly broadened matrix was obtained by convolution of the experimental spectra with compensating spread functions (Figure 9) based on the average optimum value of $k = 85$ cm^{-1} (nearly identical results were obtained with $k = 90$ cm^{-1}). PCA treatment of the compensated matrix revealed excellent adherence of combination coefficients to the α,β normalization line, justifying further correction of the spectra for very small

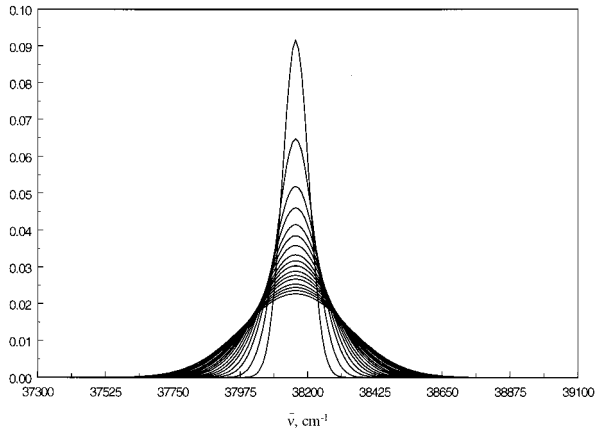

Figure 9. The series of compensating spread functions that were convolved with the experimental spectra of 1,3-butadiene.

systematic intensity errors by projecting them on the SVD α,β stoichiometric line. The smoothing effect on the second SVD eigenspectrum is dramatic (Figure 7) although somewhat less pronounced than in the simulation (Figure 2) indicating that the broadening compensation procedure may not have been fully successful.

PCA-SM treatment of the low-pressure spectra of 1,3-butadiene was based on $\Delta H^0 = 2.926$ kcal/mol, the value obtained from the onset spectra. The sum of the entropy term and the extinction coefficient term, 3.640 ± 0.122, (see Appendix, parameter -*x*(2) in eq 14) was obtained from the intercept of the van't Hoff plot. The extinction coefficient term was obtained by projection of the PCA-SM derived pure component spectra onto the SVD stoichiometric line along the CA line (for the s-trans spectrum) and the CB line (for the s-cis spectrum) in Figure 10. Intersections of these lines with the α,β stoichiometric line at points A and B define the α,β coefficients for the pure component spectra yielding the unnormalized spectra of the s-trans and s-cis conformers (Figure 11). The ratio of the integrated areas of these spectra $\sum_{\bar{\nu}}\epsilon_{\bar{\nu},\mathrm{trans}}/\sum_{\bar{\nu}}\epsilon_{\bar{\nu},\mathrm{cis}} = 1.189$ and the intercept of the van't Hoff plot give $\Delta S^0 = 3.98$ eu. Molar fractions of the two conformers as a function of *T*, based on application of the lever rule to the α,β coordinates of the spectral points on the stoichiometric line, are given in Table 2 and in Figure 12.

Discussion

The resolved *s-trans*-1,3-butadiene spectrum (band maxima at 46 500, 47 890, and 49 120 cm^{-1}) is slightly broader than the one obtained earlier without compensation for broadening, as expected.[36] Application of the differential broadening procedure to the spectrothermal matrix aims to produce a uniformly broadened matrix corresponding to the highest experimental *T* and, accordingly, the derived spectrum (Figure 11, $\lambda_{max} = 209$ nm) reflects the increase from the average effective *T* value to 93 °C. As before, with the exception of a 3 nm blue-shift and slightly better resolved vibronic progression, it is in good agreement with the spectrum assigned to this conformer in an Ar matrix at 20 K.[9] It also agrees well with the somewhat better resolved spectrum of jet-cooled 1,3-butadiene under isolated molecule conditions.[34]

The change in the *s-trans*-1,3-butadiene spectrum on decreasing *T* from 93 °C to jet-cooled conditions allows an independent test of the broadening compensation procedure developed in this work. A new spectrothermal matrix, consisting of predicted differentially broadened one-component spectra for the 93−

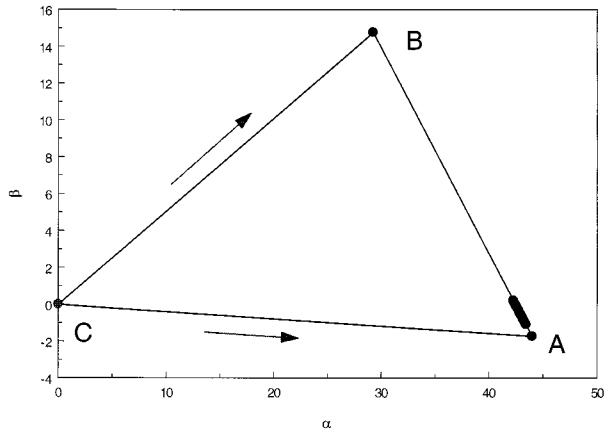

Figure 10. Projection of pure component normalized spectra along CA and CB lines on the stoichiometric line (points A − s-trans spectrum and B − s-cis spectrum).

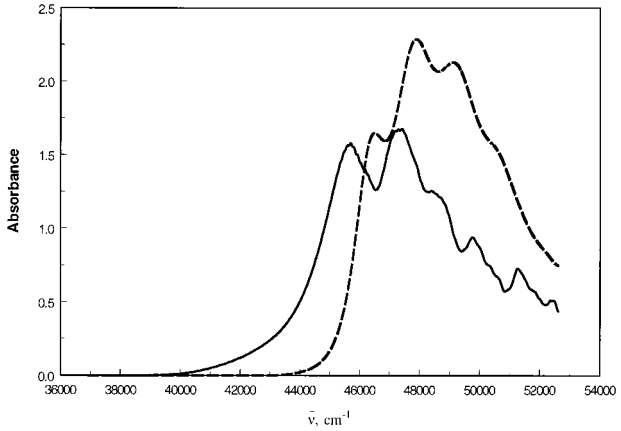

Figure 11. Pure component spectra of s-trans (dashed line) and s-cis (solid line) conformers of 1,3-butadiene obtained for $\Delta H° = 2.926$ kcal/mol.

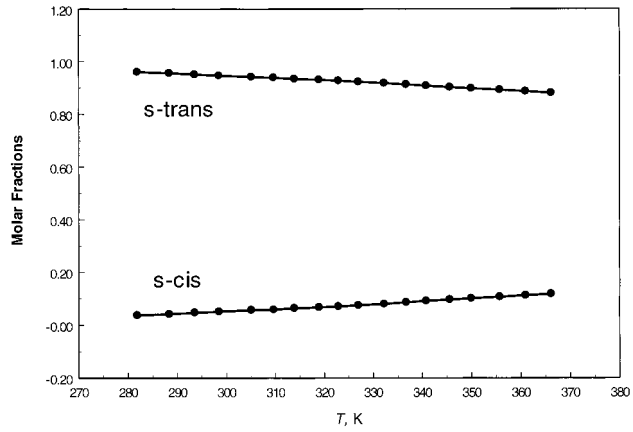

Figure 12. Molar fractions of s-cis and s-trans conformers in the experimental absorption spectra of 1,3-butadiene as a function of *T*.

178 °C range, was created by convolution of the set of Gaussians in Figure 9 with the *s-trans*-1,3-butadiene spectrum in Figure 11. SVD treatment of this matrix revealed a two-component system whose two principal eigenvectors were used to produce a best-fit approximation of the jet-cooled spectrum, by shifting the eigenvectors by 110 cm^{-1} to the red with respect to the jet-cooled spectrum. The eigenvectors, the second of which is the temperature sensitivity function, and the satisfactory result of this fit are shown in Figure 13. The 110 cm^{-1} discrepancy between our gas-phase spectra and the spectrum under jet-cooled conditions is well within experimental error. It should be noted

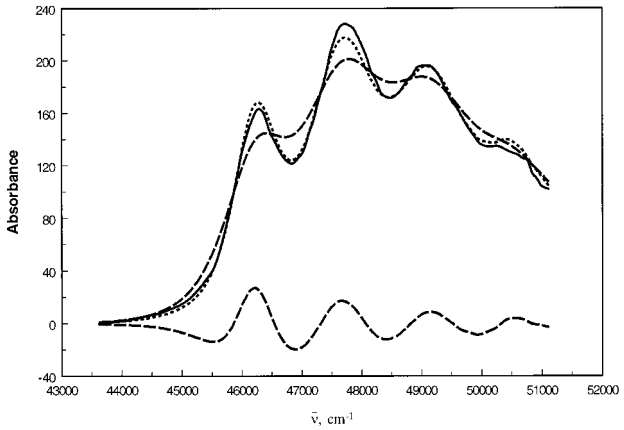

Figure 13. Extrapolated fit (short dashes) of the jet-cooled *s-trans*-1,3-butadiene spectrum (solid line) as a linear combination of SVD eigenvectors (long dashes) from a matrix generated by convolving the s-trans spectrum in Figure 11 with the spread functions in Figure 9.

that the effect of thermal broadening on the *s-trans*-1,3-butadiene spectrum is reflected in the apparent shift of the first vibronic band from 216.2 nm in the jet-cooled spectrum,[34] to 215.7 nm at −78 °C,[38] to 215.4 nm in Figure 11.

The *s-cis*-1,3-butadiene spectrum derived in this work by the broadening compensation procedure (Figures 11) is as strongly structured as the initially derived spectrum.[36] Differences due to compensation for broadening are a 1 nm blue-shift in the λ_{max} (211 nm) and a less well resolved and less intense third vibronic band. Clearly defined vibrational band progressions have been observed in the UV spectra of hexane solutions of a series of benzo[7,8]bicyclo[4.2.1]nonatrienes in which the *s-cis*-1,3-diene moiety is endocyclic in a rigid system.[39,40] However, even in this bicyclic system, decreased rigidity in the absence of the fused benzene ring leads to only slightly resolved vibrational shoulders in the UV spectrum.[39,41,42] It is also noteworthy that the UV spectra of pentane solutions of a series of *s-cis*-1,3-dienes for which the double bonds of the diene moiety are exocyclic to a C_n ring [1,2-bis(ethylidene)-cycloalkanes, $n = 4,5,6,7$] are nearly devoid of vibronic structure.[43] The λ_{max} is most blue-shifted for C_6 and C_7 for which a nonplanar diene moiety may be expected and only in the C_4 case, which should exhibit a higher degree of diene planarity, are vibronic bands clearly evident.[43] It appears that this spectral series supports Squillacote's conclusion,[9,12] that the relative positions of the λ_{max} of the UV spectra in a series of related 1,3-dienes reflect the extent to which the diene moiety deviates from planarity. Such reasoning, later challenged on theoretical grounds,[44,45] had led Squillacote to assign a gauche structure to the minor conformer of 2,3-dimethyl-1,3-butadiene in an Ar matrix at 19.5 K.[12b] Interestingly, the vibronic structure in the UV spectrum of this dimethyl derivative of *s-cis*-1,3-butadiene under the matrix conditions is better resolved than in the parent. We conclude that, while the degree of vibronic resolution in the *s-cis*-1,3-butadiene spectrum in Figure 11 may still be exaggerated, the predicted position of its λ_{max} is likely to be correct. We note here that our confidence in the validity of the differential broadening compensation method has been significantly bolstered by its successful application to the resolution of *all-trans*-1,6-diphenyl-1,3,5-hexatriene fluorescence into its three components.[46]

As noted above, a UV spectrum has been assigned to photochemically generated *s-cis*-1,3-butadiene in an Ar matrix at 20 K.[9] The λ_{max} of the s-trans spectrum in the Ar matrix at 20 K is red-shifted by 3 nm relative to that in Figure 11, and despite the much lower *T*, its vibronic structure is less well resolved than in our gas phase spectrum. The spectrum assigned to the high-energy conformer in the matrix exhibits these two effects, but in a much more pronounced manner. It is nearly devoid of vibronic structure and its λ_{max} is red-shifted 15 nm relative to ours. The large difference in response between the two conformers, taken together with the fact that the planar geometry of *s-trans*-1,3-butadiene, predicted by Hückel[1] long ago and confirmed by experimental and theoretical studies, is generally accepted, suggests a change in equilibrium geometry for the s-cis conformer on passing from the rigid matrix to the gas phase. The molecule is less planar in the gas phase, i.e., whether the higher energy conformer in the matrix is planar or not, it must be gauche in the gas phase.

Experimentally, the choice between planar and gauche structure for the geometry of *s-cis*-1,3-butadiene has been based primarily on the analysis of vibrational spectra and it has been controversial.[47−52] Analysis of recently remeasured Raman[51] and IR[52] spectra of 1,3-butadiene by Engeln et al. and by De Maré et al., respectively, supports a gauche geometry for *s-cis*-1,3-butadiene in the gas phase. Early evidence for a gauche geometry of the minor conformer was provided by temperature-dependent NMR experiments of deuterated 1,3-butadienes in CS_2 solution,[53] but large correlated errors made this conclusion unconvincing. High level ab initio and density functional calculations have generally supported the gauche geometry with a CCCC dihedral angle between 30° and 41° for the minor conformer in the gas phase.[44,45,54−60] Michl and co-workers[10,60−62] have championed a planar structure assignment on the basis of polarized IR spectra of matrix isolated *s-cis*-1,3-butadiene at low *T*. More recently, Michl et al. have also reported Ar matrix isolated 1,3-butadiene conformer Raman spectra and calculations using density functional theory and the coupled-cluster method using double substitutions.[60] A gauche geometry of the 1,3-butadiene minor conformer was now considered possible, but as a structure that tunnels very rapidly between the two mirror-image forms. The IR and Raman spectra discussed by Michl et al. are for the 1,3-butadiene conformers isolated in low *T* matrices. It is likely, therefore, that the minor conformer prefers the gauche geometry in the gas phase but adopts a nearly planar geometry in the rigid matrix. Kofranek et al. reached this conclusion by evaluation of the effect of the Ar matrix on the structure of the minor 1,3-butadiene conformer based on molecular dynamics simulations.[63]

The analysis of the simulated onset spectra shows that, despite thermal broadening, the PCA/SVD-SM treatment of the high-pressure experimental spectra allows recovery of correct thermodynamic parameters for the equilibration of the two 1,3-butadiene conformers. The derived $\Delta H°$ (320 K median *T*) of 2.93 ± 0.01 kcal/mol is in excellent agreement with our earlier value of 2.95 kcal/mol for the enthalpy difference between the two stable conformers.[36] It is also in excellent agreement with 3.02 ± 0.15 kcal/mol, the value obtained by Mui and Grunwald by attributing all absorption in the 237−249 nm region to the high energy conformer in a UV study of 1,3-butadiene gas over a much wider *T* range (298−621 K, 520 K median *T*).[37] Theoretical calculations place the energy difference in the 2.3−3.5 kcal/mol range, with many values clustering close to 3.0 kcal/mol.[45,57,58] For instance, at the G2 level of theory, Wiberg et al. obtained $\Delta\Delta H(298\ K) = 2.98$ kcal/mol for the s-trans/s-gauche equilibration.[57] Thermodynamic parameters describing the conformational equilibrium in 1,3-butadiene were calculated by Aston et al.[1c] by assuming planar stable geometries for both conformers. Compton et al. revisited these calculations and, although also expressing a preference for a planar geometry for the minor conformer, based on comparison with results obtained by Carreira,[47] obtained $\Delta H^0 = 2.7$ kcal/mol for s-trans/s-gauche equilibration (2.5 kcal/mol if the planar *s-cis*-1,3-butadiene structure were assumed instead).[49] Molar fractions of the minor conformer were estimated to vary from 0.028 to 0.069 in the 298−373 K,[49] somewhat smaller than the estimates obtained in this work (Table 2). The $\Delta S°$ (320 K median *T*) value of 3.98 eu derived from our refined treatment of the full spectra is 20% larger than the initially estimated value.[36] It is consistent with the conclusion that the gas-phase structure of the minor conformer is gauche, being larger than the $R\ln 2 = 1.38$ eu expected due to the degeneracy of the two mirror image gauche structures.

TABLE 2: Molar Fractions of the 1,3-Butadiene Conformers

T,[a] K	*s*-trans	*s*-cis (*s*-gauche)
281.91	0.9612	0.0388
288.39	0.9571	0.0429
293.61	0.9518	0.0482
298.53	0.9479	0.0521
305.15	0.9422	0.0578
309.65	0.9397	0.0603
313.95	0.9352	0.0648
318.97	0.9313	0.0687
322.87	0.9282	0.0718
326.99	0.9241	0.0759
332.25	0.9187	0.0813
336.75	0.9133	0.0867
340.85	0.9081	0.0919
345.61	0.9031	0.0968
349.95	0.8983	0.1017
355.75	0.8930	0.1070
360.95	0.8877	0.1123
366.15	0.8815	0.1185

[a] Average values for each set of five spectra; deviations from the mean ≤ 0.10 K.

The large difference in the ratio of absorptivity coefficients $(\epsilon_{s-cis}/\epsilon_{s-trans})_{max}$ of the two conformers at their respective λ_{max}, that accompanies the pronounced difference in appearance and in λ_{max} position between the spectra for the high-energy conformer obtained by Squillacote et al.[9] in a low *T* Ar matrix and by us in the gas phase, is probably due mainly to a medium imposed difference in equilibrium geometry. The value of 0.45 given by these authors is considerably smaller than 0.73, our value based on the resolved spectra in Figure 11. Although the Squillacote et al.[9] value is based on the assumption that the minor conformer is completely transparent at 207 nm and may be underestimated, the uncertainty is not sufficient to bring these ratios into agreement.

Conclusions

Application of the PCA-SM approach with the van't Hoff constraint to a spectrothermal data matrix of 1,3-butadiene onset spectra yields a very reliable $\Delta H^0_{320} = 2.93 \pm 0.01$ kcal/mol for the enthalpy difference between the two 1,3-butadiene conformers, independent of thermal spectral broadening. A procedure of broadening compensation is used in the PCA/SVD-SM resolution of the spectrothermal data matrix of full 1,3-butadiene spectra. This method makes use of the idea of compensation of thermal broadening to arrive at approximately uniform broadening in each spectrum. The form of the spread functions used resembles the form of the inhomogeneous distribution function applied elsewhere.[64] The procedure gives

resolved *s-trans*- and *s-cis*-1,3-butadiene UV spectra and molar fractions of the two components as a function of temperature. The s-trans spectrum is shown to be consistent with the spectrum obtained under jet-cooled conditions, by the use of the broadening-compensation procedure and extrapolation to low temperature. The spectrum of the minor conformer is obtained by imposing the derived $\Delta H°$ value as a constraint and depends strongly on that value. Its λ_{max} does not differ significantly from the value obtained in the initial treatment of the spectra in which the influence of thermal broadening was neglected. The position of this spectrum and the derived $\Delta S° = 3.98$ eu for conformer equilibration support the conclusion that the gas-phase structure of *s-cis*-1,3-butadiene is gauche.

Appendix

van't Hoff SM Constraint. Brief descriptions of applications of PCA-SM based on the van't Hoff plot optimization constraint are available.[16,36] We present here a more explicit description of the procedure. Self-modeling is generally carried out in the space of the combination coefficients of the eigenspectra.[13] For a two-component spectral mixture, SM is further confined to the normalization line

$$1 = \alpha_i \sum_j u_{\alpha,j} + \beta_i \sum_j u_{\beta,j} \tag{10}$$

where $u_{\alpha,j}$ and $u_{\beta,j}$ are elements of the first two PCA-derived principal eigenvectors from the matrix **U**. The values of α_i and β_i for the i_{th} experimental spectrum can be found using linear regression applied separately to each spectrum or, alternatively, using the dot products of the spectrum with each eigenvector (since $\mathbf{y}_{i,norm} = \alpha_i \mathbf{u}_\alpha + \beta_i \mathbf{u}_\beta$ then $\alpha_i = \mathbf{u}_\alpha{}^T \mathbf{y}_{i,norm}$ and $\beta_i = \mathbf{u}_\beta{}^T \mathbf{y}_{i,norm}$). Once one of the pure component spectra is located on the normalization line (for instance, using the Lawton and Sylvestre nonnegativity constraint), the search of the other pure component spectrum along the normalization line is based on the van't Hoff equation as the constraint, eq 3. In terms of spectral fractional contributions corresponding to unit area normalized spectra, this equation is

$$\ln\left(\frac{1-x_i}{x_i}\right) = -\frac{\Delta H^0}{RT_i} + \frac{\Delta S^0}{R} + \ln\frac{\sum_{\bar{\nu}} \epsilon_{\bar{\nu},cis}}{\sum_{\bar{\nu}} \epsilon_{\bar{\nu},trans}} \tag{11}$$

where

$$\frac{(1-f_i)}{f_i} = \frac{(1-x_i)}{x_i} \frac{\sum_{\bar{\nu}} \epsilon_{\bar{\nu},trans}}{\sum_{\bar{\nu}} \epsilon_{\bar{\nu},cis}} \tag{12}$$

For the butadiene case, x_i is the fractional contribution of the s-trans spectrum to the i_{th} two-component spectrum at temperature T_i, and $\sum_{\bar{\nu}} \epsilon_{\bar{\nu},trans} / \sum_{\bar{\nu}} \epsilon_{\bar{\nu},cis}$ is the ratio of the sums of the molar extinction coefficients of the two conformers over the entire applicable frequency range. The ratio of the areas of the conformer absorption spectra is a given in the simulations, but is an unknown that must be derived in the case of experimental data. Once the pure component combination coefficients are selected on the normalization line, spectral fractional contributions are defined using the lever rule

$$1 - x_i = \frac{\beta_i - \beta_{trans}}{\beta_{cis} - \beta_{trans}} \text{ and } x_i = \frac{\beta_{cis} - \beta_i}{\beta_{cis} - \beta_{trans}} \tag{13}$$

The search for the best thermodynamic parameters is based on general least squares optimization using the function $f_i(x)$, defined as the difference between the left side and the right side of eq 11, multiplied by the gas constant R

$$f_i(x) = R \ln\frac{(\beta_i - \beta_{trans})}{(\beta_{cis} - \beta_i)} + \frac{x(1)}{T_i} + x(2) \tag{14}$$

where $x(1) = \Delta H^0$ and $x(2) = -\Delta S^0 - R \ln \sum_{\bar{\nu}} \epsilon_{\bar{\nu},cis} / \sum_{\bar{\nu}} \epsilon_{\bar{\nu},trans}$.

The error function for the optimization process is defined as $^1/_2 \sum_i f_i(x)^2$ where summation runs over all introduced two-component spectra. Entering a value for β_{trans} and stepping through the values of β_{cis} allow minimization of the error function. In addition, at each step of the optimization process a van't Hoff plot is made using the current values of β_{trans} and β_{cis} and the standard deviation for the fit as a function of β_{cis} as well as the standard deviations for the slope and intercept are calculated. Although both approaches should essentially provide the same final values for the desired parameters very small discrepancies between them are encountered. In this work, the final choice of pure component combination coefficients is based on the second criterion, the van't Hoff plot optimization constraint.

The van't Hoff plot optimization constraint yields exact pure component spectra and $x(1)$, $x(2)$ parameters for the ideal simulated spectral matrix, and achieves nearly the same success for the compensated broadened spectral matrix, Figure 4. Specifically, $\Delta H^0 = 3000.16 \pm 0.19$ cal/mol (at 95% confidence level) was obtained for the latter with the correlation coefficient of the van't Hoff plot fit nearly exactly equal 1. The intercept of the plot equals 1.669 ± 0.006. Because it consists of two terms, eq 11, evaluation of ΔS^0 requires knowledge of $\sum_{\bar{\nu}} \epsilon_{\bar{\nu},cis} / \sum_{\bar{\nu}} \epsilon_{\bar{\nu},trans}$ or vice versa. The latter quantity cannot be obtained by PCA-SM, but can be readily obtained by SVD-SM employing the concept of the α,β stoichiometric line. The stoichiometric line, plane or hyperplane is analogous to the normalization line, plane or hyperplane. It was suggested by Nagle et al.[65] and then elucidated and successfully applied by Zimányi et al.[66] to determine the intermediate spectra and kinetics in the photocycle of bacteriorhodopsin. It applies to systems, as in the present conformer equilibration, for which the condition of concentration closure holds. In such cases, the abstract concentration profiles obtained directly from the SVD decomposition as $\mathbf{A} = (\mathbf{SV}^T)^T$ (where **S** is the diagonal matrix of singular values and **V** is the right singular vector matrix) play the role of the combination coefficient matrix as described in the modified Lawton−Sylvestre PCA-SM approach.[14] In this treatment, the input spectra are not normalized and stoichiometric relationships are preserved. For a two-component system, the stoichiometric line is defined by the coefficients from the first two columns of **A** and when its length is defined, the position on the line of the combination coefficients for a specific spectrum provides the values of the molar fractions of the components in the spectrum via the lever rule. The correct areas of the pure conformer spectra are obtained by projecting the normalized pure component spectra provided by the PCA-SM method onto the stoichiometric line. To this end, the normalized spectra are multiplied by a progressively increasing factor until the best correlation between the projected point and the points forming the stoichiometric line is achieved. This process can be carried out to any desired precision. In the case of the absorption spectra

the ratio of the areas of the pure component spectra projected onto the stoichiometric line is equal to $\sum_{\bar{\nu}}\epsilon_{\bar{\nu},\mathrm{cis}}/\sum_{\bar{\nu}}\epsilon_{\bar{\nu},\mathrm{trans}}$. Projection of the PCA pure component spectra for the compensated spectral matrix on the SVD stoichiometric line gives 0.472 973 for this ratio (against 0.472 648 for the ideal spectra). Substitution of this value in the expression for the intercept gives $\Delta S^0 = 3.1563$ eu, nearly identical to the input value.

Acknowledgment. This research was supported by NSF, most recently by Grant No. CHE 9985895. We are grateful to Professors R. Johnson and W. J. Leigh for private communications concerning the UV spectra of *s-cis*-1,3-diene analogues.

References and Notes

(1) (a) Hückel, E. *Z. Phys*. **1932**, *76*, 628−648. (b) Mulliken, R. S. *Rev. Mod. Phys.* **1942**, *14*, 265−274. (c) Aston, J. G.; Szasz, G.; Woolley, H. W.; Brickwedde, F. G. *J. Chem. Phys.* **1946**, *14*, 67−79. (d) Bock, C. W.; George, P.; Trachtman, M.; Zanger, M. *J. Chem. Soc., Perkin Trans. 2* **1979**, 26−34. (e) Bock, C. W.; George, P.; Trachtman, M. *Theor. Chim. Acta* **1984**, *64*, 293−311.

(2) (a) Havinga, E. *Chimia* **1962**, *16*, 145−172. (b) Jacobs, H. J. C.; Havinga, E. *Adv. Photochem*. **1979**, *11*, 305−373. (c) Jacobs, H. J. C.; Gielen, J. W. J.; Havinga, E. *Tetrahedron Lett.* **1981**, *40*, 4013−4016. (d) Jacobs, H. J. C.; Gielen, J. W. J.; Havinga, E. *J. Photochem*. **1981**, *17*, 3−3.

(3) Liu, R. S. H.; Turro, N. J.; Hammond, G. S. *J. Am. Chem. Soc.* **1965**, *87*, 3406−3412.

(4) Dilling, W. L.; Kroering, R. D.; Little, J. C. *J. Am. Chem. Soc*. **1970**, *92*, 928−948.

(5) Saltiel, J.; Metts, L.; Sykes, A.; Wrighton, M. *J. Am. Chem. Soc*. **1971**, *93*, 5302−5303.

(6) Srinivasan, R. *J. Am. Chem. Soc*. **1968**, *90*, 4498−4499.

(7) (a) Boue, S.; Srinivasan, R. *J. Am. Chem. Soc*. **1970**, *92*, 3226−3227. (b) Saltiel, J.; Metts, L.; Wrighton, M. *J. Am. Chem. Soc*. **1970**, *92*, 3227−3228.

(8) Vanderlinden, P.; Boue, S. *J. Chem. Soc., Chem. Commun.* **1975**, 932−933.

(9) Squillacote, M. E.; Sheridan, R. S.; Chapman, O. L.; Anet, F. A. L. *J. Am. Chem. Soc*. **1979**, *101*, 3657−3658.

(10) Arnold, B. R.; Balaji, V.; Michl, J. *J. Am. Chem. Soc*. **1990**, *112*, 1808−1812.

(11) Liu, R. S. H.; Hammond, G. S. *Proc. Nat. Acad. Sci., USA* **2000**, *97*, 11 153−11 158.

(12) (a) Squillacote, M. E.; Semple, T. C. *J. Am. Chem. Soc*. **1990**, *112*, 5546−5551. (b) Squillacote, M. E.; Semple, T. C.; Mui, P. W. *J. Am. Chem. Soc*. **1985**, *107*, 6842−6846.

(13) (a) Lawton, W. H.; Sylvestre, E. A. *Technometrics* **1971**, *13*, 617−633. (b) Sylvestre, E. A.; Lawton, W. H.; Maggio, M. S. *Technometrics* **1974**, *16*, 353−368.

(14) (a) Sun, Y.-P.; Sears, D. F., Jr.; Saltiel, *J. Anal. Chem*. **1987**, *59*, 2515−2519. (b) Sun, Y.-P.; Sears, D. F., Jr.; Saltiel, J.; Mallory, F. B.; Mallory, C. W.; Buser, C. A. *J. Am. Chem. Soc.* **1988**, *110*, 6974−6984. (c) Saltiel, J.; Sears, D. F., Jr.; Choi, J.-O.; Sun, Y.-P.; Eaker, D. W. *J. Phys. Chem.* **1994**, *98*, 35−46. (d) Saltiel, J.; Choi, J.-O.; Sears, D. F., Jr.; Eaker, D. W.; O'Shea, K. E.; Garcia, I. *J. Am. Chem. Soc.* **1996**, *118*, 7478−7485.

(15) Aartsma, T. J.; Gouterman, M.; Jochum, C.; Kwiram, A. L.; Pepich, B. V.; Williams, L. D. *J. Am. Chem. Soc.* **1982**, *104*, 6278−6283.

(16) Sun, Y.-P.; Sears, D. F., Jr.; Saltiel, J. *J. Am. Chem. Soc.* **1989**, *111*, 706−711.

(17) Ghiggino, K. P.; Skilton, P. F.; Fischer, E. *J. Am. Chem. Soc.* **1986**, *110*, 1146−1149.

(18) (a) Spalletti, A.; Bartocci, G.; Masetti, F.; Mazzucato, U.; Cruciani, G. *Chem. Phys.* **1992**, *160*, 131−144. (b) Bartocci, G.; Mazzucato, U.; Spalletti, A. *Chem. Phys*. **1996**, *202*, 367−376.

(19) Saltiel, J.; Choi, J.-O.; Sears, D. F., Jr.; Eaker, D. W.; Mallory, F. B.; Mallory, C. W. *J. Phys. Chem*. **1994**, *98*, 13162−13170.

(20) (a) Saltiel, J.; Zhang, Y.; Sears, D. F., Jr.; Choi, J.-O. *Res. Chem. Interm.* **1995**, *21*, 899−921. (b) Saltiel, J.; Zhang, Y.; Sears, D. F., Jr. *J. Phys. Chem. A.* **1997**, *101*, 7053−7060.

(21) Jones, H. C.; Strong, W. W. *The Absorption Spectra of Solutions*, Carnegie Institute: Washington, 1911: pp 9−70.

(22) (a) Sklar, L. A.; Hudson, B. S.; Petersen, M.; Diamond, *J. Biochemistry* **1977**, *16*, 813−828. (b) Andrews, J.; Hudson, B. S. *J. Chem. Phys*. **1978**, *68*, 4587−4594. (c) Hudson, B. S.; Kohler, B. E.; Schulten, K. In *Excited States*; Lim, E. C., Ed. Academic Press: New York, 1982; Vol. 6, pp 1−95. (d) Itoh, T.; Kohler, B. E. *J. Phys. Chem.* **1987**, *91*, 1760−1764.

(23) Bourne, B.; Burgess, C. *Analyst* **1995**, *120*, 2075−2080.

(24) Nodland, E.; Libnau, F. O.; Kvalheim, O. M.; Luinge, H.-J.; Klaeboe, P. *Vib. Spectrosc.* **1996**, *10*, 105−123.

(25) Nodland, E,; Libnau, F. O.; Kvalheim, O. M. *Vib. Spectrosc*. **1996**, *12*, 163−176.

(26) Penner, S. S. *Quantitative Molecular Spectroscopy and Gas Emissivities*, Addison-Wesley: Reading, Massachusetts, 1959.

(27) Jansson, P. A. In *Deconvolution of Images and Spectra*; Academic Press: New York, 1997; pp 42−75.

(28) Hochstrasser, R. M. *Acc. Chem. Res.* **1968**, *1*, 266−274.

(29) Jortner, J.; Rice, S. A.; Hochstrasser, R. M. *Adv. Photochem*. **1969**, *7*, 149−309.

(30) Simons, J. P. *J. Phys. Chem*. **1984**, *88*, 1287−1293.

(31) (a) Maeda, Y.; Okada, T.; Noboru, N.; Irie, M. *J. Phys. Chem.* **1984**, *88*, 1117−1119. (b) Maeda, Y.; Okada, T.; Mataga, N.; *J. Phys. Chem*. **1984**, *88*, 2714−2718.

(32) Dogonadze, R. R.; Itskovitch, E. M.; Kuznetsov, A. M.; Vorotyntsev, M. A. *J. Phys. Chem*. **1975**, *79*, 2827−2834.

(33) Ulstrup, J.; Jortner, J. *J. Chem. Phys*. **1975**, *63*, 4358−4368.

(34) Leopold, D. G.; Pendley, R. D.; Roebber, J. L.; Hemley, R. J.; Vaida, V. *J. Chem. Phys.* **1984**, *81*, 4218−4229.

(35) Itskovitch, E. M.; Ulstrup, J.; Vorotyntsev, M. A. In *The Chemical Physics of Solvation*; Dogonadze, R. R., Kalman, E., Kornyshev, A. A., Ulstrup, J., Eds.; Elsevier: Amsterdam, 1985; pp 223−310.

(36) Sun, Y.-P.; Sears, D. F., Jr.; Saltiel, J. *J. Am. Chem. Soc*. **1988**, *110*, 6277−6278.

(37) (a) Mui, P. W.; Grunwald, E. *J. Am. Chem. Soc.* **1982**, *104*, 6562−6566. (b) Mui, P. W.; Grunwald, E. *J. Phys. Chem*. **1984**, *88*, 6340−6344.

(38) McDiarmid, R. *Chem. Phys. Lett.* **1975**, *34*, 130−134.

(39) Johnson, R. P. *Ph.D. Dissertation*, Syracuse University, Syracuse, New York, 1976.

(40) (a) Hahn, R. C.; Johnson, R. P. *Tetrahedron Lett.* **1973**, 2149−2152. (b) Hahn, R. C.; Johnson, R. P. *J. Am. Chem. Soc*. **1975**, *97*, 212−213.

(41) C. W. Jefford, C. W.; Burger, U.; Delay, F. *Helv. Chim. Acta* **1973**, *56*, 1083.

(42) Footnote 105 in ref 39.

(43) (a) Postigo, J. A. *Ph.D. Thesis*, McMaster University, Hamilton, Ontario, Canada, 1995. Avail. University Microfilms Int., Order No. DANN05893; *Diss. Abstr. Int. B* **1996**, *57*, 1804. (b) Leigh, W. J.; Postigo, J. A. *J. Chem. Soc., Chem. Commun*. **1993**, 1836−1838.

(44) Bock, C. W.; Panchenko, Y. N. *J. Mol. Struct.* **1989**, *187*, 69−82.

(45) Guo, H.; Karplus, M. *J. Chem. Phys.* **1991**, *94*, 3679−3699.

(46) Turek, A. M.; Sears, D. F., Jr.; Garcia, I.; Saltiel, J. Manuscript in preparation.

(47) Carreira, L. A. *J. Chem. Phys*. **1975**, *62*, 3851−3854.

(48) Durig, J. R.; Bucy, W. E.; Cole, A. R. H. *Can. J. Phys*. **1975**, *53*, 1832−1837.

(49) Compton, D. A. C.; George, W. D.; Maddams, W. F. *J. Chem. Soc., Perkin 2* **1976**, 1666−1671.

(50) Furukawa, Y.; Takeuchi, H.; Harada, I.; Tasumi, M. *Bull. Chem. Soc. Jpn*. **1983**, *56*, 392−399.

(51) Engeln, R.; Consalvo, D.; Reuss, J. *Chem. Phys*. **1992**, *160*, 427−433.

(52) De Maré, G. R.; Panchenko, Y. N.; Auwera, J. V. *J. Phys. Chem. A* **1997**, *101*, 3998−4004.

(53) Lipnick, R. L.; Garbisch, E. W., Jr. *J. Am. Chem. Soc*. **1973**, *95*, 6370−6375.

(54) Alberts, I. L.; Schaefer, H. F.; III *Chem. Phys. Lett.* **1989**, *161*, 375−382.

(55) Szalay, P. G.; Lischka, H.; Karpfen, A. *J. Phys. Chem.* **1989**, *93*, 6629−6631.

(56) Wiberg, K. B.; Rosenberg, R. E.; Rablen, P. R. *J. Am. Chem. Soc*. **1991**, *113*, 2890−2898.

(57) Murcko, M. A.; Castejon, H.; Wiberg, K. B. *J. Phys. Chem*. **1996**, *100*, 16162−16168.

(58) Karpfen, A.; Choi, C. H.; Kertesz, M. *J. Phys. Chem*. **1997**, *101*, 7426−7433.

(59) Senent, M. L. *J. Mol. Spectr*. **1998**, *191*, 265−275.

(60) Choi, C. H.; Kertesz, M.; Dobrin, S.; Michl, J. *Theor. Chem. Acc*. **1999**, *102*, 196−206.

(61) Fisher, J. J.; Michl, J. *J. Am. Chem. Soc*. **1987**, *109*, 1056−1059.

(62) Arnold, B. R.; Balaji, V.; Downing, J. W.; Radziszewski, J. G.; Fisher, J. J.; Michl, J. *J. Am. Chem. Soc*. **1991**, *113*, 2910−2919.

(63) Kofranek, M.; Karpfen, A.; Lischka, H. *Chem. Phys. Lett*. **1992**, *189*, 281−286.

(64) Litvinyuk, I. V. *J. Phys. Chem. A* **1997**, *101*, 813−816.

(65) Nagle, J. F.; Zimányi, L.; Lanyi, J. K. *Biophys. J*. **1995**, *68*, 1490−1499.

(66) (a) Zimányi, L.; Kulcsár, Á.; Lanyi, J. K.; Sears, D. F., Jr.; Saltiel, J. *Proc. Natl. Acad. Sci. U.S.A.* **1999**, *96*, 4408−4413. (b) Zimányi, L.; Kulcsár, Á.; Lanyi, J. K.; Sears, D. F., Jr.; Saltiel, J. *Proc. Natl. Acad. Sci. U.S.A.* **1999**, *96*, 4414−4419.